In Vivo Muscle Stiffening Under Bone Compression Promotes Deep Pressure Sores

A. Gefen

N. Gefen

E. Linder-Ganz

Department of Biomedical Engineering,
Faculty of Engineering,
Tel Aviv University,
Tel Aviv, Israel
e-mail: gefen@eng.tau.ac.il

S. S. Margulies

Department of Bioengineering,
University of Pennsylvania,
Philadelphia, Pennsylvania

Pressure sores (PS) in deep muscles are potentially fatal and are considered one of the most costly complications in spinal cord injury patients. We hypothesize that continuous compression of the longissimus and gluteus muscles by the sacral and ischial bones during wheelchair sitting increases muscle stiffness around the bone-muscle interface over time, thereby causing muscles to bear intensified stresses in relentlessly widening regions, in a positive-feedback injury spiral. In this study, we measured long-term shear moduli of muscle tissue in vivo in rats after applying compression (35 KPa or 70 KPa for $1/4$–2 h, $N=32$), and evaluated tissue viability in matched groups (using phosphotungstic acid hematoxylin histology, $N=10$). We found significant (1.8-fold to 3.3-fold, $p<0.05$) stiffening of muscle tissue in vivo in muscles subjected to 35 KPa for 30 min or over, and in muscles subjected to 70 KPa for 15 min or over. By incorporating this effect into a finite element (FE) model of the buttocks of a wheelchair user we identified a mechanical stress wave which spreads from the bone-muscle interface outward through longissimus muscle tissue. After 4 h of FE simulated motionlessness, 50%–60% of the cross section of the longissimus was exposed to compressive stresses of 35 KPa or over (shown to induce cell death in rat muscle within 15 min). During these 4 h, the mean compressive stress across the transverse cross section of the longissimus increased by 30%–40%. The identification of the stiffening-stress-cell-death injury spiral developing during the initial 30 min of motionless sitting provides new mechanistic insight into deep PS formation and calls for reevaluation of the 1 h repositioning cycle recommended by the U.S. Department of Health. [DOI: 10.1115/1.1894386]

Keywords: Bedsores, Decubitus Ulcers, Immobilization, Soft Tissue Injury, Muscle Biomechanics

Introduction

Pressure sores (PS) are the consequence of intense and prolonged mechanical loading of vascularized soft tissues, which causes cell death through metabolic deprivation [1–3] and/or critical deformation [4]. Immobilization and lack of sensory feedback are the greatest risk factors for PS onset [5] and accordingly, spinal cord injury (SCI) patients are among the most vulnerable populations [6]. Despite considerable efforts to minimize the prevalence of this malady among SCI patients, almost one-third of these patients develop at least one PS during their initial acute care and rehabilitation, and between 15% and 26% of the patients develop a PS thereafter [6]. These complications cause pain, suffering, and longer hospitalization time for SCI patients. Additionally, PS impose vast healthcare costs, e.g., around 1.2 billion dollars are invested annually in treating SCI-related PS alone [7]. Worse still, PS are potentially fatal such as in the recent death of movie star Christopher Reeve in October of 2004. Septicemia and severe infectious complications associated with PS are considered the major direct causes of death [8,9].

Two different mechanisms for onset of PS were recently recognized [10]: (i) Superficial (mild) PS (types I, II) are caused by friction and shear stresses between the body and supports. The shearing stresses cause superficial tissue breakdown that is exacerbated by moisture and elevated temperature and (ii) Deep (severe) PS in vascularized tissues (typically skeletal muscles) are produced by tissue compression under bony prominences resulting in local obstructions or occlusions in blood supply for a critical time period [1–3]. These ischemic conditions, together with critical prolonged deformation of tissues, may result in cell death in the affected tissues. In early stages, these deep PS cannot be identified by examination of the skin, which often leads to progress to a more serious injury level before detection. Thus, these deep PS are costly to treat, and are considered a heavy burden in managing SCI patients.

Deep PS in SCI patients typically appear in the muscles padding the sacrum and ischial tuberosities—the longissimus and gluteus muscles—likely because of the denser vascularization in striated muscles compared with that in more superficial tissues [10–12]. Clinical evidence of deep muscle injury in immobilized patients [11,12] is consistent with animal studies in which compression of soft tissue layers composed of skin, subcutaneous fat, and striated muscles initially manifested cell death in muscle tissue. Specifically, Daniel et al. [2] showed that in pigs, pressure of 67 KPa delivered for 4 h was sufficient to cause muscle cell death, but skin injury required application of 107 KPa for 8 h. Moreover, muscle layers directly envelope highly curved bone surfaces (e.g., under the sacrum and ischial tuberosities) that, from a biomechanical perspective, tend to concentrate loads and mechanical stresses. Hence, it is not surprising that when a multilayered soft tissue structure (including skin, subcutaneous fat, soft connective tissues, and muscles) is loaded by the body weight which compresses it between the supporting surfaces (e.g., wheelchair cushion) and curved bony prominences (e.g., the sacrum), pathologic changes associated with ischemia are likely to appear first in muscle tissue.

The biomechanical factors which determine the risk for deep PS onset are twofold, extrinsic and intrinsic. Important extrinsic factors, for example, are the mechanical properties of the supports (e.g., stiffness, friction coefficient), which influence the contact

Contributed by the Bioengineering Division for publication In the JOURNAL OF BIOMECHANICAL ENGINEERING. Manuscript received August 12, 2004; revision received December 23, 2004. Associate Editor: Michael Sacks.

loads to which the body is subjected. Important intrinsic factors are the geometry and mechanical properties of the soft tissue layers that are compressed between the supports and bony prominences during wheelchair sitting. The individual combination of anatomy and tissue stiffness characteristics determines the intensity of loads to which deep tissues are exposed for given wheelchair and sitting position. In view of the susceptibility of muscular tissue to PS, its mechanical properties are of particular interest. Specifically, long-term viscoelastic properties of muscular tissue should be studied, because PS develop on a time scale of minutes to hours [1–4], during which stress relaxation occurs in the tissue under body-weight loading.

We hypothesize that mechanical properties of striated muscle tissue play an important role in the etiology of deep PS characteristic to SCI patients. It is widely recognized that isolated soft tissue specimens stiffen gradually post-mortem (e.g., ligaments [13], intervertebral discs [14], and brain [15]). The stiffer mechanical behavior of dead tissues was attributed to cellular decomposition resulting in the rise in the swelling pressure of the tissue [16], to intracellular proteolysis [17] or to rigor mortis in muscles [18]. In a novel hypothesis we propose that stiffening may also occur in vivo in muscular tissue which underwent widespread cell death produced by applied bone compression. Furthermore we hypothesize that local cell-death-related stiffening will affect the distribution of mechanical stresses and deformations in adjacent (not yet damaged) muscular tissue, further promoting deep PS.

In a previous study, we found abnormal (1.6-fold) stiffening ($p<0.05$) of rat gracilis muscles that were exposed to external compression (35 KPa–70 KPa for 2–6 h) in vivo and then tested in uniaxial tension in vitro, at strains of 2.5%–7.5% [19]. In that study, exposure of rat gracilis to 11.5 KPa did not induce histological evidence of damage or abnormal mechanical properties even in cases where pressure was delivered continuously for 6 h. The goals of this study are to (i) measure the viscoelastic mechanical properties of rat skeletal muscles in vivo before and after delivery of prolonged compression (applied for up to 2 h), (ii) compare changes in muscle mechanical properties with histological damage, and (iii) characterize the effect of abnormal stiffening of muscle properties on the biomechanical conditions for onset and progression of deep PS in sitting humans, using a computational model of the buttocks of a wheelchair (SCI) user.

Methods

Mechanical Testing. Striated muscle tissue is a hierarchial structure containing packed muscle fibers that are enveloped by endomysium thin connective tissue and bundled together by perimysial connective tissue. This heterogeneous structure generally exhibits anisotropic material behavior, but for the purpose of biomechanical measurements, it is common to approximate muscle tissue as being a homogenous and isotropic material [20,21]. This assumption allows for evaluation of stiffness of muscle tissue in vivo.

In order to measure viscoelastic mechanical properties of rat muscles in vivo we employed the well-established indentation method [22–26]. This method utilizes a rigid indentor that is pressed against the tissue by a force $P(t)$ [N] deflecting the tissue $\delta(t)$ [mm]. Corresponding to our selection of an indentor with a hemispherical tip of radius $R=2$ [mm] (to avoid sharp edges that may cause microtears in the tissue during testing), we applied the solution of Lee and Radok [27], which provides the viscoelastic shear modulus $G(t)$ [MPa] of the tested material, assuming that the material occupies a semi-infinite elastic space

$$G(t) = \frac{3P(t)}{16\delta(t)\sqrt{R\delta(t)}} \qquad (1)$$

The indentor's radius (R) is an important parameter of the indentation test which should be adequately selected. Zheng et al. [28] conducted experiments on fresh fish tissue to optimize the indentor's size for the thickness of the sample, and concluded that R should be equal or less than 25% the thickness of the studied sample. This also ensures that unintended misalignment of the indentor that is smaller than 12.5 deg will have a negligible effect on the measured mechanical properties. For testing gracilis muscle of adult rats, which is typically 15–20 mm thick, an indentor with radius of $R=2$ mm is appropriate.

The displacement $\delta(t)$ is determined to be of a "ramp-and-hold" wave shape, i.e., the indentor is pressed into the tissue at a velocity of 1 mm/s until reaching a depth of 1 mm, where it is held in depth for 50 s. Because this study focuses on formation of PS, which is a gradual, slow process occurring under a nearly constant load (i.e., body weight of the immobilized patient), we report the long-term shear modulus of muscles G_∞. Consistently, we indented at a moderate speed, 1 mm/s, to measure the load-relaxation response in rat muscles that reflects the consequence of a moderate soft tissue deformation rate by a person's self body weight while sitting down (or being seated) on a wheelchair.

In order to simultaneously measure the indentation force and displacement, an electromechanical, computer-controlled and precalibrated indentor, comprising a miniature linear stepper motor (min. displacement 0.0032 mm), force transducer (max. load 1.47 N or 150 g) and a linear variable displacement transducer was used (Fig. 1).

Experimental Protocol. Pressures measured to occlude blood flow in subcutaneous tissues over the ischial tuberosities were around 40 to 50 KPa [29]. Our finite element (FE) analysis of the buttocks described later on shows that compression stresses of that order, and even greater, develop in the longissimus and gluteus muscles of humans during motionless sitting. With respect to exposure time, a study monitoring sitting paraplegic subjects equipped with pressure transducers over each ischial tuberosity showed that subjects who moved every 10 min or less did not develop PS [30], but according to the U.S. Department of Health, PS develop within 2 h of immobilization [31]. Taking this literature and our present FE simulations together, our animal study was designed to apply combinations of constant pressure magnitudes (35, 70 KPa) and exposure durations (15 min–2 h) that will potentially cause PS in muscles of animal models. Rats, a well-established animal model for studying soft tissue tolerance to pressure injuries [19,32–35], were selected for this study. We produced PS in the rat's gracilis muscle (an adductor of the thigh), because it is relatively large and flat and is conveniently accessible for mechanical testing after reflection of the skin.

The following protocol was approved by the Institutional Animal Care and Use Committees of the University of Pennsylvania (No. 708193) and of Tel Aviv University (No. M-03-109). A total number of 42 Sprague-Dwaley mature (3–4 month-old) male rats (weight 280 ± 20 g) were assigned for this study (Table 1): 32 rats were assigned for G_∞ in vivo measurements, and the additional ten were assigned for muscle histology which is described later. The group assigned for G_∞ testing was further divided into eight subgroups, each comprising four animals. In these eight subgroups, the gracilis muscles were surgically exposed and subjected to the following pressure-time combinations (Table 1): (1) 35 KPa for 15 min; (2) 35 KPa for 1/2 h; (3) 35 KPa for 1 h; (4) 35 KPa for 2 h; (5) 70 KPa for 15 min; (6) 70 KPa for 1/2 h; (7) 70 KPa for 2 h; and, (8) no pressure applied. This experimental design (Table 1) considered delivery of comparable pressure doses (PD, the time-pressure integral) between some pairs of experimental groups to investigate whether the PD, used in clinical evaluation of diabetic plantar tissue [36], can also be employed to predict the extent of damage to muscle tissue during PS onset. Specifically, PD of 17.5 KPa h was delivered to rats exposed to 35 KPa for 1/2 h and to rats exposed to 70 KPa for 1/4 h. Likewise, equivalent PD of 35 KPa h was delivered to rats exposed to 35 KPa for 1 h and to rats exposed to 70 KPa for 1/2 h.

Rats were anesthetized using ketamine (90 mg/Kg) and xyla-

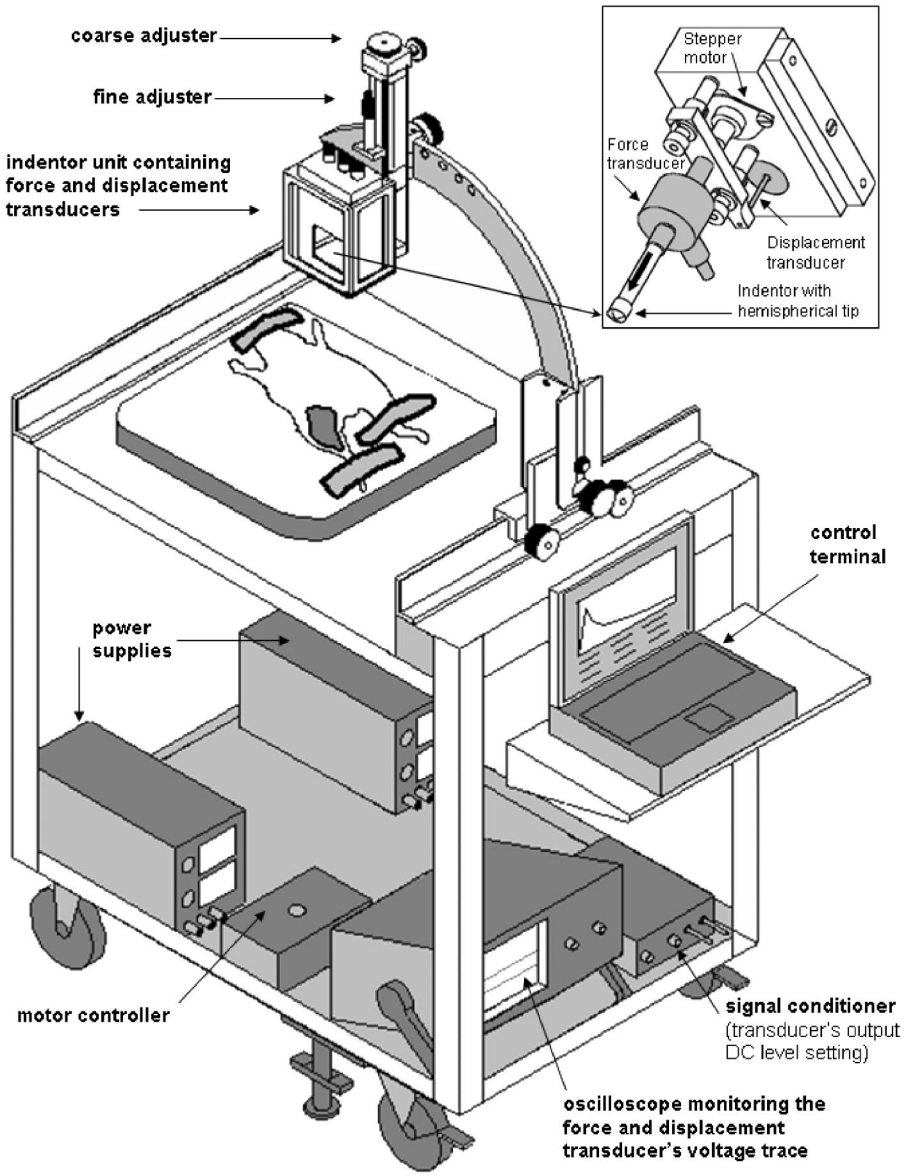

Fig. 1 Scheme of the computer-controlled indentation system for measuring long-term shear modulus G_∞ of rat muscle tissue

Table 1 Sizes of experimental groups

Pressure delivered	Animals assigned for	Duration of pressure delivery				Number of animals
		1/4 h	1/2 h	1 h	2 h	
35 KPa	G_∞ Measurements	4	4	4	4	16
	Histology	2	2			4
70 KPa	G_∞ Measurements	4	4	-	4	12
	Histology	2				2
Controls	Time-matched surgical controls					4
	Histology					4

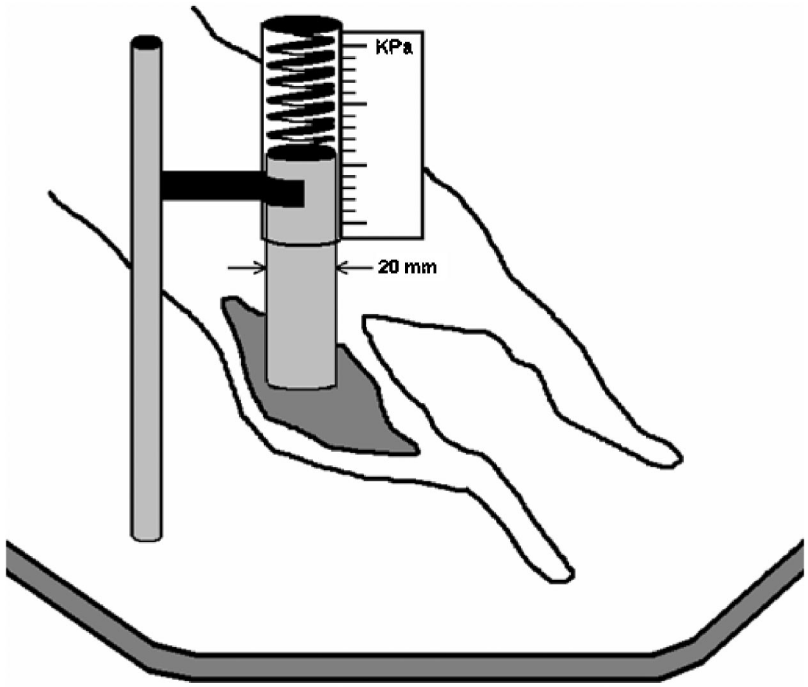

Fig. 2 Scheme of the compression apparatus used to induce pressure injury on the exposed rat muscle tissue

zine (10 mg/Kg) that were intraperitonially injected, and 1/3 of this dose was used for maintenance of anesthesia during experiments. Depth of anesthesia was verified by lack of pinch response. Hair of the hind limb (randomized, left or right) was carefully shaved and the skin over the proximal lateral part of the limb was reflected using a scalpel to expose the gracilis. Special care was taken not to damage muscular tissue during surgery. Exposed muscle tissue was maintained moist at all times using spray of saline.

Long-term shear moduli G_∞ of the gracilis were measured at three time points: (i) before delivery of pressure to the exposed gracilis (baseline stage); (ii) immediately after delivery of pressure (post-compression stage); and (iii) 30 min after pressure was removed (reperfusion stage) to detect potential recovery of abnormal G_∞ after reperfusion of the muscle. The 30 min recovery time was selected to represent potential muscle recovery in a wheelchair user who optimally follows the recommendations of the U.S. Department of Health, and changes his/her sitting posture every less than one hour [31].

To acquire G_∞ measurements at baseline stage, the rat femur was firmly fixed to the rigid support under the indentor using heavy-duty adhesive tapes at the ankle and knee joints (Fig. 1). Next, the indentor was positioned using its fine system of adjustments until delicate contact was made with the surface of the exposed gracilis muscle, as determined by monitoring the force transducer's signal on an oscilloscope (Fig. 1). In preliminary testing of the indentation system while pressing the indentor against the center of a digital scale, we measured the threshold of detectable contact at a force of 0.02 g, which can be considered as the consistent preload in all the present indentation tests. The surface of the gracilis was indented at a velocity of 1 mm/s to a depth of 1 mm. The indentor was then held in depth for 50 s during which muscle-indentor contact force data were continuously acquired on a computer at 25 Hz (Lab View 6i, National Instruments). Although for the study of PS injury, nonpreconditioned (NPC) G_∞ data appear to be the most relevant (because once an immobilized patient was positioned, he is not expected to change posture for a long time), we also acquired preconditioned (PC) shear moduli for completeness. Therefore, each 1 mm indentation was performed five times, designating the first indentation maneuver as the non-preconditioned run. According to Carew et al. [37], preconditioning without adequate rest periods between subsequent loading cycles increases predictive errors, and therefore, a pause of 20 s between subsequent test runs was used to allow elastic recovery of the muscle tissue.

Next, in groups (1)–(7), pressure was applied directly on the gracilis. For that purpose, rats were placed within a specially designed apparatus which comprised a spring-derived rigid plastic compressor (diameter 20 mm) which delivered precalibrated constant compression to the muscle's surface (Fig. 2). During delivery of pressure, the limb was fixed to the base of the apparatus using heavy-duty adhesive tapes at the knee and ankle. Immediately after delivery of pressure, animals were returned to the indentation system for post-compression G_∞ measurements, and were then kept under anesthesia for 30 min of reperfusion, followed by another session of G_∞ measurements. At each experimental stage (baseline, post-compression, reperfusion) we repeated the indentation measurements at three adjacent sites on the muscle's surface, running five preconditioning indentation maneuvers at each site to obtain naive, non-preconditioned as well as preconditioned G_∞ values. Intra-animal variability of G_∞ moduli across adjacent sites on the muscle's surface was in the order of 10% (ratio of standard deviation to the mean) for baseline testing, and in order of 15% after pressure was delivered. Accordingly, we averaged G_∞ results across site at each stage (baseline, post-compression, and reperfusion) to reduce variability. Sites of indentation were marked with a permanent color marker and were photographed for documentation. After completing measurements of G_∞ at the three stages of the experiment, animals were euthanized with an overdose of pentobarbital and death was verified by cessation of heartbeat.

Group (8) was assigned as time-matched control animals for the surgical procedure (Table 1). In this group, G_∞ of the gracilis were measured in three adjacent sites immediately after skin was reflected, and again 1/2 h, 1 h, 1 1/2 h, 2 h, and 2 1/2 h after skin reflection without any delivery of pressure, to eliminate effects of muscle dehydration on measured G_∞. Muscles of time-matched surgical controls were kept moist using saline spray in the same manner by which muscles exposed to pressure were treated. After acquiring G_∞ data over time, these animals were also euthanized with overdose of pentobarbital.

Statistical Analysis. To allow a nondimensional statistical analysis of changes in muscle stiffness, we defined property ratios of shear moduli for the compression $\overline{G}_\infty^{\text{comp}}$ and reperfusion $\overline{G}_\infty^{\text{reper}}$ stages of the experiment with respect to the baseline shear modulus value

$$\overline{G}_\infty^{\text{comp}} = \frac{G_\infty^{\text{comp}}}{G_\infty^{\text{baseline}}} \tag{2}$$

$$\overline{G}_\infty^{\text{reper}} = \frac{G_\infty^{\text{reper}}}{G_\infty^{\text{baseline}}} \tag{3}$$

where $G_\infty^{\text{baseline}}$ is the baseline long-term shear modulus, G_∞^{comp} is the long-term shear modulus post-compression [Eq. (2)] and G_∞^{reper} is the long-term shear modulus after 30 min of reperfusion [Eq. (3)]. It follows from these definitions [Eqs. (2) and (3)] that (i) properties remain unaffected if the mean property ratio of an experimental group is statistically indistinguishable from unity, and that (ii) muscle tissue abnormally stiffens if the mean property ratio is significantly greater than unity.

Paired one-tail *t*-test between $\overline{G}_\infty^{\text{comp}}$ and unity was employed for each experimental group to determine if statistically significant tissue stiffening occurred. Based on previous published experimental data showing consistent, statistically significant increase in muscle tissue stiffness post-compression [19], one-tail testing was selected to increase the statistical power of these tests. Power analysis (paired, $\alpha=0.05$, 0.9 power) was run to determine the minimal detectable difference in comparison of $\overline{G}_\infty^{\text{comp}}$ to unity for the only group that did not show statistically significant stiffening of moduli (as reported in the Results section)—the group exposed to 35 KPa for 15 min ($N=4$).

Next, we used property ratios [Eq. (2) and (3)] to test the effect of muscle reperfusion by comparing $\overline{G}_\infty^{\text{comp}}$ and $\overline{G}_\infty^{\text{reper}}$ within each group using a paired two-tail *t*-test (the more conservative two-tail test was used here because no previous data on the effect of reperfusion on moduli were available). Finally, we conducted pairwise multiple comparisons of $\overline{G}_\infty^{\text{comp}}$ property ratios across experimental groups using a post-hoc Fisher's least-significant-difference test. We further verified the results from the Fisher's analysis with a Dunnett test for multiple comparisons of $\overline{G}_\infty^{\text{comp}}$ property ratios from all experimental groups with unity. For each test type, preconditioned and nonpreconditioned property ratios were analyzed separately. For all the above statistical tests, a *p* value less than 0.05 was considered significant.

Histological Evaluation. The ten animals assigned for histological evaluation were divided into four sub-groups. In these four subgroups, the gracilis muscles were surgically exposed and subjected to the following pressure-time combinations (Table 1): 35 KPa for 15 min ($N=2$); 35 KPa for 1/2 h($N=2$); 70 KPa for 15 min ($N=2$); and histology controls not subjected to pressure ($N=4$). Histological evaluation was conducted only for the above specific pressure-time combinations because (i) in all these short-time (15, 30 min) exposures, cell death was already evident (as detailed in the Results section) and so, we stopped further animal sacrifices assuming that a longer exposure to the same pressure magnitudes will also result in cell death, and (ii) because long-time (2 h) exposures were previously reported to induce cell death [19]. The surgical procedure to expose the gracilis was identical to that carried out in preparation for G_∞ measurements (see Experimental Protocol). Two cubic samples (face length ~10 mm) were harvested from the gracilis muscle at the site exposed to pressure. For muscles which were subjected to pressure, samples were extracted immediately after delivery of pressure to allow the histology findings to be associated with G_∞ measurements taken (from different animals) at equivalent times (during the post-compression stage). In preparation for tissue slicing, specimens were fixed in formaline. Slicing was carried out perpendicularly to the direction of load, at thickness of 5 μm (diameter of a muscle fiber in the rat is ~30 μm). All slices were studied. Sections were mounted on glass slides and stained with phosphotungstic acid hematoxylin (PTAH) in order to study cell viability and integrity of cross striation [19].

Computational Model. In order to determine the effects of stiffening of muscular tissue under bone compression *in humans* we employed a three-dimensional (3D) computational model of a transverse 1-cm slice through the buttocks [Fig. 3(*a*)]. Using the FE method (NASTRAN 2003), we solved the model for the distribution of internal principal compression stresses in the soft tissues surrounding the pelvic and sacral bones during wheelchair sitting [Fig. 3(*b*)]. Subsequently, we obtained the time-dependent changes in the state of stresses due to modified muscle tissue G_∞ properties that were observed in the animal studies. The methodology of FE model development is described in detail in [19]. For completeness, a brief description of its essential components follows.

The transverse two-dimensional (2D) geometry of a cross section through the buttocks was obtained from the "Visible Human" (male) digital database, and transferred to a solid modeling software package (SOLIDWORKS 2003) for detection and segmentation of cortical and trabecular bone of the pelvis and sacrum, cartilage, fat, skin, muscles (longissimus and gluteus), internal organs (colon and ileum), and major blood vessels. The 2D cross section was then extruded 1 cm along the transverse direction to form a 3D model [Fig. 3(*a*)]. The buttocks model was supported by an elastic cushion (thickness: 15 cm; elastic modulus: 150 KPa; friction coefficient between the skin and cushion: 0.4 [38]). The foundation of the cushion was fixed for translational and rotational displacements. The analysis considered the weights of all tissues, the abdominal pressure and the skeletal forces (F_1, F_2) and skeletal moments (M_1, M_2) that are transfered through the spine during sitting for two different backrest angles, 70 deg and 80 deg [Fig. 3(*b*)]. The musculoskeletal loads F_1, F_2, M_1, M_2 (Table 2) were calculated for each backrest inclination case from static equilibrium of the free-body-diagram of the entire slice (as described in the Appendix of [19]).

The model was meshed into 16,664 tissue elements and 3847 cushion elements [Fig. 3(*c*)]. All tissues and the cushion were considered homogeneous and isotropic materials. Skin and fat, which undergo large deformation during sitting, were assumed to be nonlinear elastic materials. Bone, cartilage, colon, and ileum tissues were assumed to behave linear elastically. Constitutive relations for all tissues excluding skeletal muscle tissue were as specified in [19]. To model the viscoelastic response of muscle tissue under constant (body-weight) loading, we employed the principle that a viscoelastic, time-dependent mechanical behavior approaches elastic behavior at long times. For the purpose of biomechanical modeling, it is practical to consider muscle tissue as a linear viscoelastic material, which allows calculation of the transient shear modulus $G(t)$ from [39]

$$G(t) = (G_\infty - G_i)(1 - e^{-t/\tau}) + G_i \tag{4}$$

where G_∞ is the long-term shear modulus, G_i is the instantaneous shear modulus (immediately after deformation has ceased), and τ is the time constant of relaxation. Our stress relaxation indentation experiments showed that muscle tissue reached a stable relaxation

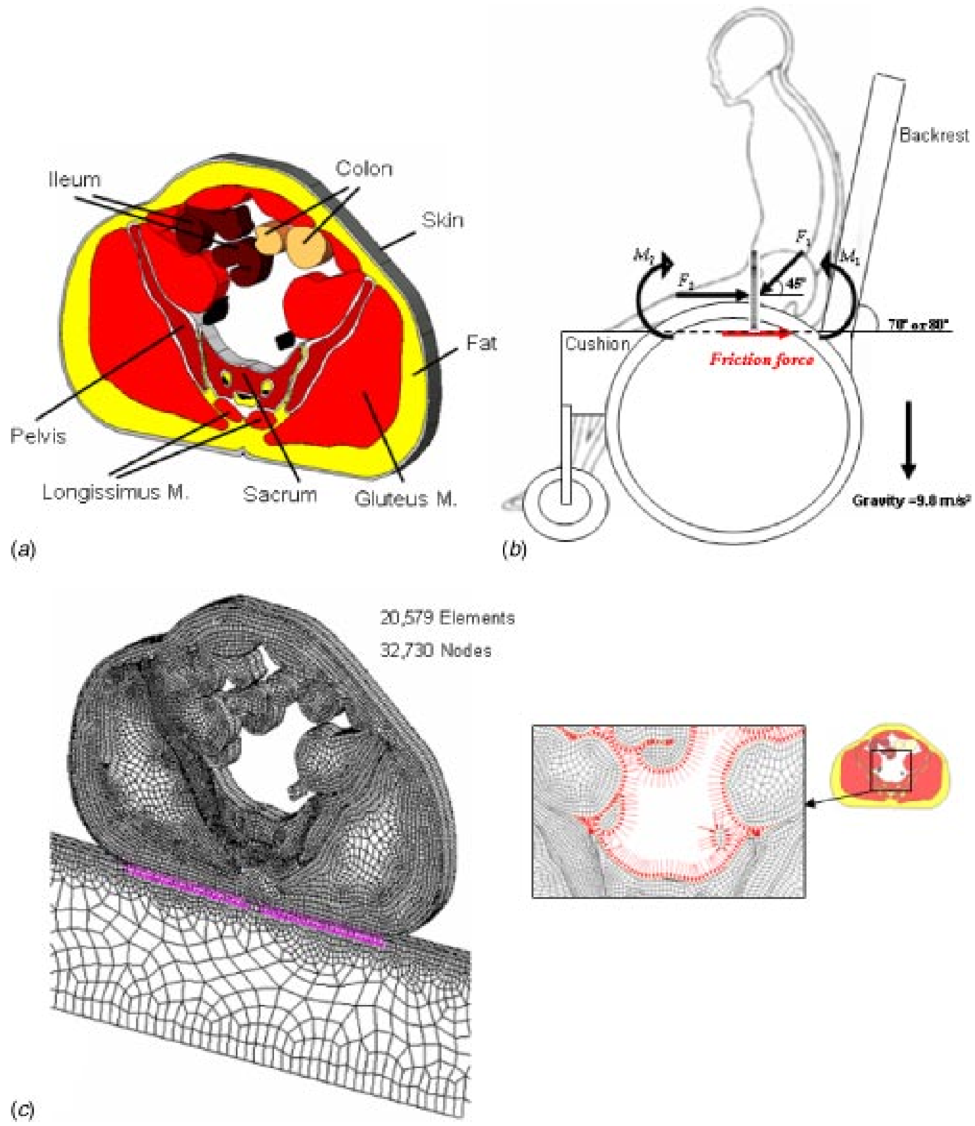

Fig. 3 Computational modeling of the buttocks during wheelchair sitting: (*a*) three-dimensional solid model, (*b*) free-body-diagram showing the system of skeletal forces (F_1, F_2), skin-cushion friction force and skeletal moments (M_1, M_2) acting on the model, and (*c*) finite element meshing with magnification of the abdominal cavity region subjected to abdominal pressure

response (i.e., the "long-term phase" of the relaxation curve) after 40 s to 45 s. The time scale for the present FE analyses, however, was in the order of 15 min (900 s) between subsequent simulation steps (consistent with our animal study design in which shortest exposure to pressure was 15 min) which is ~20-fold the relaxation time. Accordingly, for the purpose of FE analysis of the buttocks during prolonged continuous sitting, muscle tissue can be considered to reach its elastic long-time behavior G_∞ at each simulation step. The dependence of G_∞ on the magnitude of deformation in large deformations (nonlinearity) was not accounted for in the present FE modeling because of the lack of experimental data regarding the influence of PS on nonlinearity.

Model predictions of contact stress between the buttocks and the support surface during sitting were validated using contact pressure measurements ("Flexiforce" sensors, Tekscan Co., Boston, MA, thickness 0.13 mm; range: 0 N–4.4 N, accuracy: ±5%).

Table 2 Loading system for the finite element model of the buttocks during wheelchair sitting, corresponding to the diagram in Fig. 3(*b*). The loads applied to the slice through the buttocks include skeletal forces (F_1, F_2), skin-cushion friction forces and skeletal moments (M_1, M_2) for two backrest inclination angles. The method of calculation is described elsewhere [19].

Backrest inclination	F_1 [N]	F_2 [N]	Friction f [N]	M_1 [Nm]	M_2 [Nm]
70 deg	320	336	111	63	68
80 deg	220	247	66	32	35

Table 3 Means, standard deviations (SD), and p values of property ratios for experimental groups (compared with unity within each group). $\bar{G}_{\infty}^{\mathrm{comp}}$=Long-term shear modulus after compression normalized by the baseline long-term shear modulus; $\bar{G}_{\infty}^{\mathrm{reper}}$=Long-term shear modulus after reperfusion normalized by the baseline long-term shear modulus; NS =not significant.

Group		$\bar{G}_{\infty}^{\mathrm{comp}}$ Nonpreconditioned			$\bar{G}_{\infty}^{\mathrm{comp}}$ Preconditioned			$\bar{G}_{\infty}^{\mathrm{reper}}$ Nonpreconditioned			$\bar{G}_{\infty}^{\mathrm{reper}}$ Preconditioned		
Pressure (KPa)/Time (1H)		Mean	SD	p	Mean	SD	p	Mean	SD	p	Mean	SD	p
35	1/4	1.21	0.39	NS	1.17	0.37	NS	0.99	0.25	NS	0.90	0.12	NS
35	1/2	1.87	0.41	0.01	1.77	0.38	0.01	1.72	0.21	0.00	1.64	0.29	0.01
35	1	2.39	1.23	0.04	1.95	0.62	0.03	2.09	0.68	0.02	1.80	0.57	0.03
35	2	3.29	1.73	0.04	2.85	1.24	0.03	2.40	0.76	0.02	2.12	0.49	0.01
70	1/4	2.54	1.07	0.03	2.20	0.93	0.04	1.99	0.48	0.01	1.71	0.37	0.02
70	1/2	3.01	0.70	0.01	2.85	0.75	0.01	2.73	0.64	0.01	2.53	0.64	0.01
70	2	3.28	1.56	0.03	3.10	1.54	0.04	2.73	0.64	0.01	2.65	0.78	0.01

The ischial bones of volunteer subjects (five female and five males, age: 27±2, weight: 69±10 Kg, height: 175±9 cm) were located by palpation and three pressure sensors were adhered to the body under each ischium. Subjects sat on a flat rigid surface covered by the same elastic cushion considered in the FE model. Using an unpaired t test, we verified that the peak contact pressure predicted by our FE model under the ischial bones (20 KPa) was statistically indistinguishable from measured peak contact pressures under ischial bones of subjects (mean ± standard deviation: 18±6 KPa, $p<0.05$). Detailed sensitivity analysis of the model was included in [19]. Briefly, body weight had the most influential effect (an additional 40 Kg of body weight increased peak compressive stress in the longissimus by 89%); peak stress predictions deviated within a range of ~7% in response to a ±20% change in skin and fat stiffness, and to a ±25% change in muscle stiffness [19].

To account for time-dependent changes in G_{∞} of muscle tissue under compression as shown in our present animal studies, we first analyzed the distribution of compression stress in muscle tissue of the computer model. In each site where simulated compression stress equaled or exceeded a compression level that was shown to stiffen G_{∞} of rat muscles, we increased G_{∞} of muscle tissue at that specific site of the computer model, by the corresponding stiffening factor that was obtained experimentally (as described later; factors provided in Table 3). For example, G_{∞} of muscle elements that were subjected to compression stress of more than 70 KPa in the computer model was increased 2.54-fold (just for these elements) in order to mimic local stiffening of muscle tissue subjected to that extent of compression for 1/4 h. Fisher's least-significant-difference tests showed that $\bar{G}_{\infty}^{\mathrm{comp}}$ of muscles exposed to 35 KPa for 2 h were statistically indistinguishable from those of muscles exposed to 35 KPa for 1 h, and likewise, $\bar{G}_{\infty}^{comp}$ of muscles exposed to 70 KPa for 2 h were indistinguishable from those of muscles exposed to 70 KPa for 1/2 h. Plotting the stiffening factors in Table 3 on a time scale (separately for 35 KPa and 70 KPa exposures) shows that both nonpreconditioned and preconditioned factors approach asymptotic values at long times. We therefore assumed that stiffening factors for muscle elements in the FE analyses at times longer than 2 h were the same as the 2 h factors (Table 3).

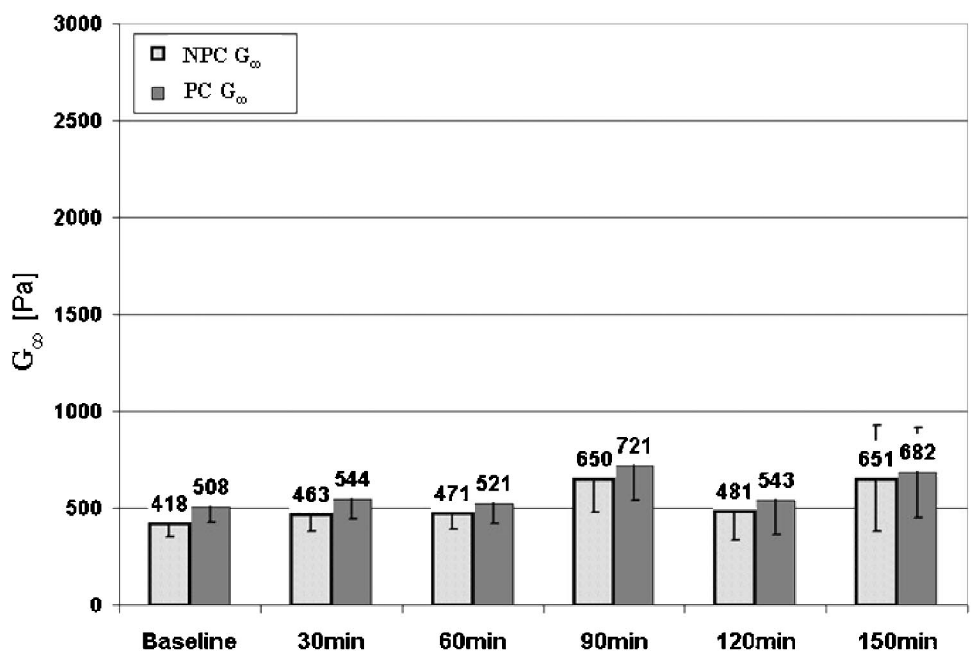

Fig. 4 Nonpreconditioned (NPC) and preconditioned (PC) long-term shear moduli G_{∞} of gracilis muscle of surgical control rats over time (N=4), from time of skin reflection (baseline). No pressure was applied on muscles of this group.

Results

Mechanical Testing. Long-term shear moduli G_∞ of surgical controls (subgroup 8) over time (up to 150 min from the time of skin reflection) were generally similar to baseline values (Fig. 4). A mild increase in muscle stiffness appeared 90 min after surgery (significant for PC $\overline{G_\infty}$ with respect to unity, $p=0.045$), likely because of some tissue dehydration, but at 120 min and 150 min, stiffening was again insignificant (Fig. 4). Overall, we conclude that the surgical procedure of skin reflection did not affect muscle stiffness within the first hour, and may had a mild effect ($\sim$1.4-fold increase in NPC $\overline{G_\infty}$ and $\sim$1.3-fold increase in PC $\overline{G_\infty}$; Fig. 4) at 90 min and thereafter.

G_∞ post-compression (G_∞^{comp}) were significantly greater than baselines in all experimental groups ($p<0.05$) except the one in which the gracilis was subjected to 35 KPa for 15 min [Fig. 5(*a*)]. Likewise, except for 35 KPa applied for 15 min, after allowing 30 min of reperfusion of the compressed muscle (G_∞^{reper}) G_∞ were significantly greater than baselines values, indicating that muscle stiffness did not spontaneously recover to baseline level with reperfusion after a significant increase in stiffness had occurred. Across experimental groups, both G_∞^{comp} and G_∞^{reper} consistently increased with time of exposure to pressure (up to 3.3-fold, Fig. 5, and Table 3). In all experimental groups but the 35 KPa for 15 min, the extent of stiffening (minimum: 1.8-fold after 30 min; maximum: 3.3-fold after 2 h; Table 3) was greater than the maximal stiffening observed in the surgical controls (1.4-fold after 90 min), approving that pressure was indeed the cause for tissue stiffening. Property ratios (NPC and PC) of compressed ($\overline{G_\infty^{\text{comp}}}$) and reperfused ($\overline{G_\infty^{\text{reper}}}$) muscles were significantly greater than unity $p<0.05$ in a one-tail t test for $\overline{G_\infty^{\text{comp}}}$ and in a two-tail t test for $\overline{G_\infty^{\text{reper}}}$ for all groups but the one subjected to a pressure of 35 KPa for 15 min (Table 3). According to the power analysis, the design of the present study was adequate to determine significant differences greater than 0.6 between $\overline{G_\infty^{\text{comp}}}$ and unity. Thus, we cannot exclude a possibility that the difference between $\overline{G_\infty^{\text{comp}}}$ and unity in the 35 KPa 15 min group might have been statistically significant in a larger study population.

Property ratios of reperfused muscles were almost always indistinguishable from those immediately post-compression, however, in two groups a slight (but statistically significant) recovery of muscle stiffness was identified: PC moduli from the group subjected to 35 KPa for 1 h decreased by $\sim$8% (mean) with reperfusion, and similarly, PC moduli from the group subjected to 70 KPa for 30 minutes decreased by $\sim$11% with reperfusion.

Fisher's multiple comparisons detected significant stiffening of muscles following 2 h of exposure to 35 KPa ($p<0.01$), but exposure to 35 KPa for 1 h or less did not result significant stiffening. Likewise, this test detected significant stiffening after 30 min ($p<0.01$) and after 2 h ($p<0.01$) of exposure to 70 KPa, but exposure to 70 KPa for just 15 min was not sufficient to manifest a significant change according to Fisher's. Hence, a Fisher's analysis indicates that significantly abnormal properties manifest during the second hour of exposure to 35 KPa, and between 15 min and 30 min of exposure to 70 KPa. A Dunnett test yielded results that were consistent with those of the Fisher's analysis.

Pressure doses were shown to be ineffective in predicting the extent of abnormal increase in muscle stiffness. Specifically, PD of 17.5 KPa h caused 1.9-fold stiffening of muscles in the group exposed to 35 KPa for 1/2 h, but the same PD caused 2.5-fold stiffening in the group exposed to 70 KPa for 1/4 h (Table 3). Similarly, PD of 35 KPa h caused 2.4-fold stiffening of muscles in the group exposed to 35 KPa for 1 h, but the same PD caused three-fold stiffening in the group subjected to 70 KPa for 1/2 h. We conclude that the pressure magnitude and exposure time parameters should be specified separately for predicting muscle tissue stiffening under compression.

Histological Evaluation. Death of muscle cells and loss of cross striation were demonstrated with PTAH staining in all experimental groups that were assigned for histology (35 KPa delivered for 1/4 h (Fig. 6), 35 KPa delivered for 1/2 h and 70 KPa delivered for 1/4 h). In frames where cell death was apparent, 30% to 90% of the frame area contained dead muscle tissue. None of the control slides included such abnormalities, and so, we conclude that tissue damage was induced by mechanical compression in our experimental protocol. Injuries were generally dispersed across the cross section of the muscle, with dead muscle fascicles being adjacent to viable fascicles. In all experimental groups, some transitional regions of partially viable tissue were identified (Fig. 6). Since rat muscle tissue subjected to 35 KPa for 15 min demonstrated cell death and loss of cross striation but did not manifest significant changes in mechanical properties, and since in all other groups both histological and mechanical property abnormalities were demonstrated, we conclude that cell death and structural changes (such as loss of cross-striation) precede changes in mechanical properties.

Computational Model. Peak principal compressive stresses in the longissimus muscles during wheelchair sitting with the backrest inclined 80 deg (5700 KPa) and 70 deg (4000 KPa) were 292-fold and 266-fold greater than peak contact pressures, respectively. Likewise, peak compressive stresses in the gluteus muscles with the backrest inclined 80 deg (1830 KPa) and 70 deg (1460 KPa) were 96-fold and 94-fold greater than peak contact pressure, respectively, confirming that interfacial pressures are inefficient measures for predicting conditions for deep PS onset [19]. Muscle tissue during wheelchair sitting is generally subjected to large deformations, e.g., when the backrest of the wheelchair was inclined 80 deg, peak strains in the longissimus and gluteus were 10.4% and 12.9%, respectively. Peak principal compressive stresses at both the longissimus and gluteus muscles during sitting (with backrest inclinations of 70 deg and 80 deg) exceeded 70 KPa (Fig. 7). Therefore, these simulations predict that sitting postures will stiffen deep muscle tissue at the overstressed sites after 15 min of motionlessness. Consequently to stiffening, stress levels at the stiffened sites and in surrounding tissue rise. This triggers a detrimental positive-feedback mechanism of increase in tissue stiffness and subsequent increase of stress levels in the muscles, which was manifested in the present simulations as a *stress wave* that propagates from the sacral bone outward through longissimus tissues (Fig. 8). The greater backrest inclination angle (80 deg) produced a more intense and faster stress wave (Fig. 8). For backrest inclination of 80 deg, we found that muscle regions subjected to compressive stress of 35 KPa or over expanded in area by 35% after 1/4 h and by 60% after 4 h of motionless wheelchair sitting. During that time, the mean compressive stress across the transverse cross section of the longissimus increased 1.43-fold. For backrest inclination of 70 deg, we found that muscle regions subjected to compression stress of 35 KPa or over expand in area by 25% after 1/4 h and by 52% after 4 h of motionless sitting, and within the 4-h time frame, the mean compressive stress in the longissimus increased 1.3-fold.

Discussion

This study characterized basic pathophysiological and biomechanical phenomena in the onset of PS. Specifically, using an animal model of deep PS under a bony prominence, we demonstrated significant stiffening (1.8-fold to 3.3-fold, $p<0.05$ in one-tail t tests) of muscle tissue in vivo in groups subjected to 35 KPa for 30 min or over, and in all groups subjected to 70 KPa. In all experimental groups, substantial cell death occurred in the muscle region that was subjected to pressure. Interestingly, all statistical tests resulted that the slight increase in gracilis stiffness for the

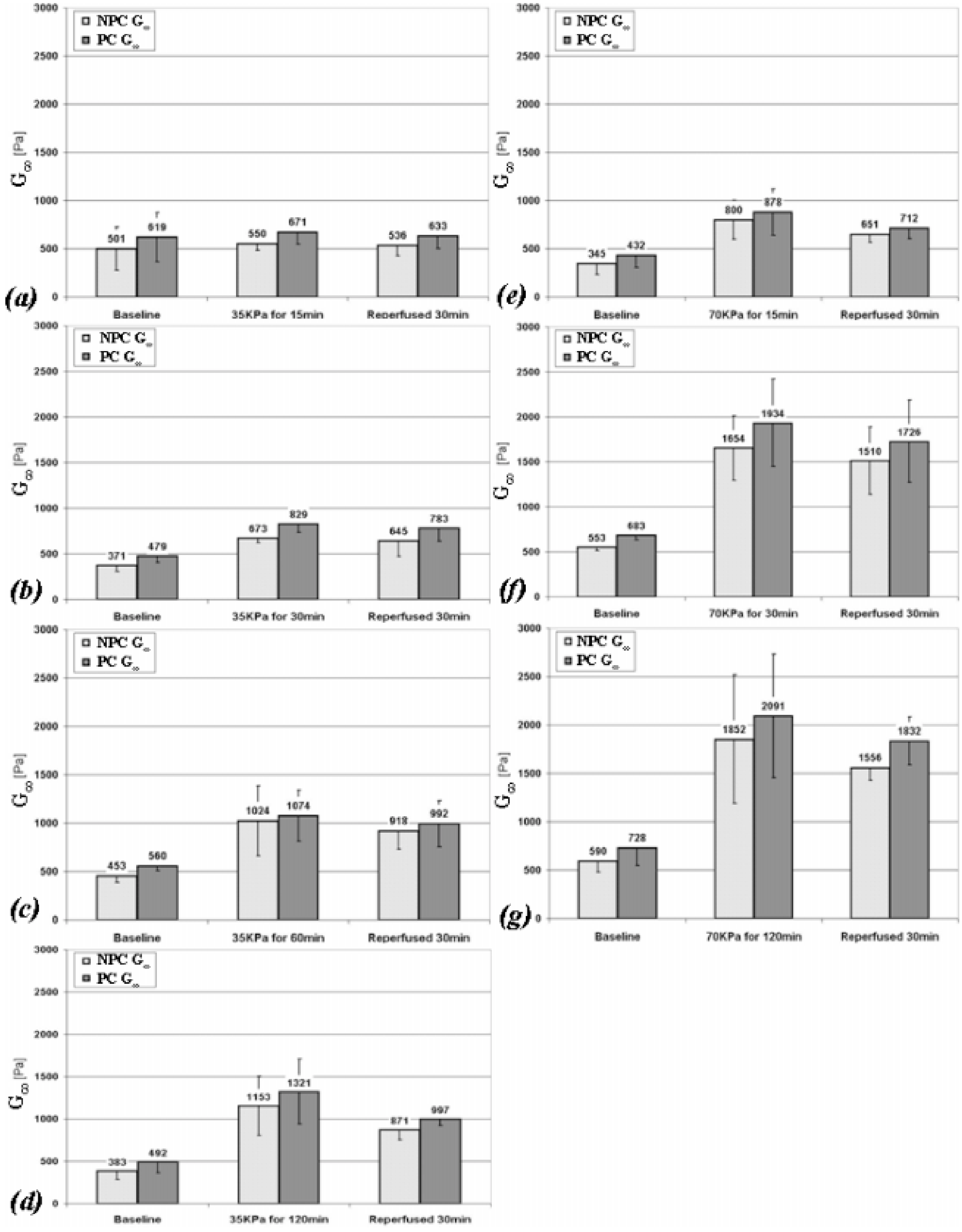

Fig. 5 **Nonpreconditioned (NPC) and preconditioned (PC) long-term shear moduli G_∞ of gracilis muscle of rats subjected to pressure of 35 KPa for (*a*) 15 min, (*b*) 30 min, (*c*) 60 minutes, and (*d*) 120 min, and of rats subjected to 70 KPa for (*e*) 15 min, (*f*) 30 min and (*g*) 120 min. Bars indicate means and vertical lines indicate standard deviations. For each group (N=4 in each) the baseline shear modulus (immediately after skin reflection), post-compression modulus, and modulus after 30 mins of reperfusion are depicted.**

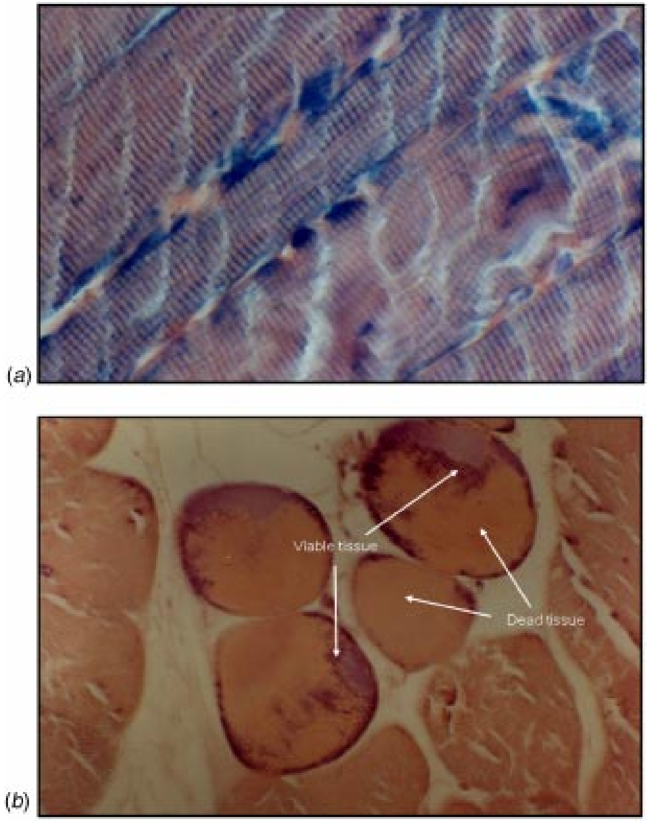

Fig. 6 Representative phosphotungstic acid hematoxylin (PTAH) staining of (*a*) control rat gracilis muscle tissue (not subjected to pressure), showing a clear cross-striation structure stained blue by PTAH, and of (*b*) muscle tissue which was subjected to compression of 35 KPa for 15 min. Injuries in (*b*) are dispersed, with dead muscle fascicles (not stained, and no cross striation) being adjacent to viable fascicles (stained blue, and cross-striation maintained). Within the frame shown in (*b*), ~88% of the area of muscle tissue contained dead cells. Magnification was set as X300.

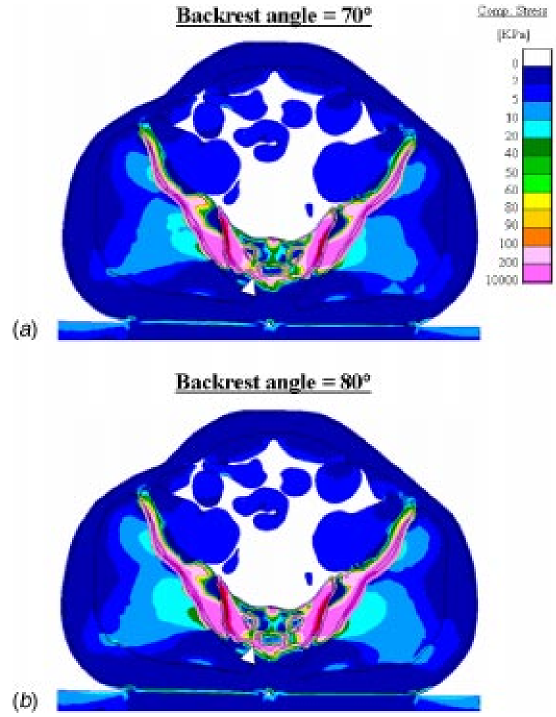

Fig. 7 Model predictions of distributions of principal compressive stresses in the buttocks during wheelchair sitting with the backrest of the wheelchair inclined (a) 70 deg and (b) 80 deg with respect to the horizon. Arrowheads indicate locations of peak principal compressive stress (in the right longissimus muscle, adjacent to the sacrum).

animal group exposed to 35 KPa for 15 min (~9% for NPC and PC properties) was insignificant, but a histological evaluation of this group indicated that the tissue was partially dead (Fig. 6). Based on the results from this group we conclude that significant changes in mechanical properties follow extensive morphological damage and cellular death, and not vice versa. Therefore, future development of noninvasive techniques for diagnosis and prognosis of deep PS based on mechanical property distribution (e.g., using ultrasound-based or MRI-based tissue elastography methods, reviewed in [40]) may employ elevated muscle stiffness as a marker of already existing damage, but not as a predictor of potential damage.

The FE model of the buttocks during immobilized wheelchair sitting (characteristic to SCI) demonstrated that: (1) deep muscles which pad the pelvic and sacral bones during sitting (longissimus, gluteus) are subjected to stresses that are greater by two orders of magnitude than corresponding buttocks-wheelchair interfacial stresses (Fig. 7), and therefore, the common clinical practice of monitoring interfacial pressures in order to protect SCI patients from PS may have fundamental flaws; and (2) abnormal stiffening of muscle tissue *in vivo* under compression may play a key role in spreading of deep PS. The injured, stiffer muscle tissue bears elevated stresses, and projects these stresses to adjacent tissue that was not yet injured, thereby exposing it to potentially damaging loads. This may drive a positive-feedback mechanism in which elevated stresses in widening regions around the bone-muscle interface (Fig. 8) increase the potential for cell death in muscle tissue. For wheelchair users, the simulations predicted that peak muscle stresses during sitting can be moderately reduced when the backrest inclination is reduced, e.g., reducing the backrest angle from 80 deg to 70 deg reduced the peak compressive stress in the longissimus from 5700 KPa to 4000 KPa, but still, after 15 min of immobilized sitting ~25% of the cross-sectional area of this muscle was subjected to potentially injuring stresses (⩾35 KPa). We conclude that merely decreasing the backrest inclination is an insufficient intervention for relief of elevated buttocks stresses in wheelchair-bounded patients.

Reperfusion of muscle tissue for 30 min after the tissue was continuously compressed never recovered muscle stiffness back to baseline in all cases where immediately after tissue compression, stiffness was significantly above baseline. Although a very mild (but statistically significant) decrease in stiffness (~10%) was observed after allowing reperfusion in two experimental groups, considering also the histological findings, the experimental data indicate occurrence of permanent damage. This suggests that if tissue stiffening (following cell death) already took place, patient repositioning to relieve tissue loads may delay, but cannot terminate the positive-feedback deterioration mechanism. Widening of regions which bear potentially injuring stresses is expected to continue as soon as the injuring posture recurs.

In a previous study of rat (gracilis) muscle stiffness following exposure of the muscle to continuous pressures we delivered pressures in vivo and then, harvested the muscles for in vitro testing [19]. In vitro, we placed the harvested muscles under uniaxial tension (along the direction of the muscle fibers) using an electromechanical universal testing machine (Instron 5544). Using this in vitro testing configuration we demonstrated statistically significant stiffening following exposure to pressures of 35 KPa or 70 KPa (for 2 h to 6 h), but stiffness increased more moderately than in

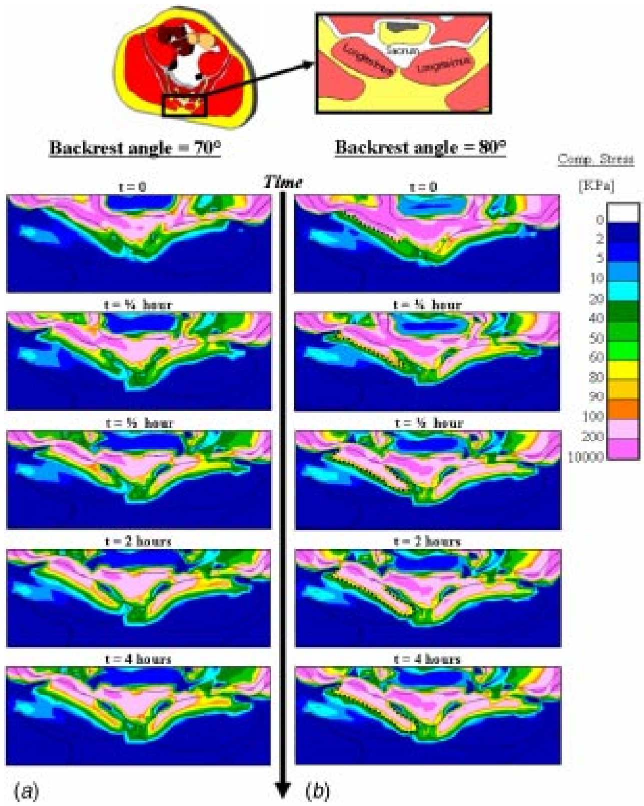

Fig. 8 Finite element model predictions of the time-dependent distribution of principal compression stresses in the longissimus muscle during wheelchair sitting. Based on our animal studies, muscle tissue elements subjected to compressive stresses σ_c in the range 35 KPa $\leqslant \sigma_c <$ 70 KPa stiffen (by factors specified in Table 3) after 1/2 h of immobilized sitting. Stiffening of muscle tissue at sites subjected to $\sigma_c \geqslant$ 70 KPa occurs after just 15 min of immobilized sitting (Table 3). For simulation case (*a*), where the backrest inclination is 70 deg, 28% of the cross-sectional area of the longissimus is subjected to potentially injuring stresses ($\geqslant$35 KPa) after 15 minutes of immobilized sitting. For simulation case (*b*), where the backrest inclination is 80 deg, 35% of the cross-sectional area of muscle tissue is susceptible to injury after 15 min of immobilization. The dotted line in each time frame of the stress analysis shows the propagation and widening of the 70 KPa stress wave within the right longissimus.

the present study, to 1.6-fold that of controls [19]. We consider the more dramatic increase in stiffness manifested in the present study (1.8-fold to 3.3-fold stiffening) to be more relevant than the results from our previous uniaxial testing (1.6-fold stiffening) for analysis of deep PS in humans. This is not only because presently, muscles were tested in vivo (and so, no post-mortem rigor state effects could have been involved), but also because in the present study, muscles were tested under compressive loading (of indentation) in the transverse direction. Loading the rat gracilis transversally to the direction of the muscle fibers and measuring its stiffening response in that direction conform the in vivo condition in seated humans. In seated humans, the longissimus and gluteus muscles are loaded by the sacrum and ischial tuberosities transversally to the direction of fibers, and therefore, the muscle mechanical properties relevant to PS in these muscles are the transverse ones, which characterize how pressures of the bony prominences are being resisted (or cushioned) by the muscles. The present study specifically provided the transverse stiffness of muscle tissue and its dependence on the loading history in the transverse direction.

Very little information is available in the literature regarding passive viscoelastic mechanical behavior of living or fresh muscle tissue from humans. Specifically, there is paucity of data regarding directional transverse elastic or shear moduli for living/fresh human muscles. In vitro tensile tests of fresh human muscle fibers incidentally extracted during surgical treatment of trauma (e.g., from the brachioradialis, thumb, and wrist extensors) showed that the longitudinal elastic modulus was $E=28\pm3$ KPa (mean ± standard deviation) [41]. Considering that muscle tissue contains mostly water ($\sim$75%) and therefore, is nearly incompressible (Poisson's ratio ν approaches 0.5), shear moduli can be approximated from $G=E/2(1+\nu)$, as $\sim$9 KPa. In vivo measurements obtained with ultrasound-based or MR-based elastography are in good agreement with this estimate. Shear moduli of unloaded human muscle tissue obtained using elastography for the lateral gastrocnemius [42,43], biceps brachii [43,44], flexor digitorum profundus [43], and soleus [43] are in the ranges of 5 KPa to 20 KPa, and standard deviations are around 5 KPa to 8 KPa. Only one paper used elastography to study in vivo directional properties of muscle tissue [45], and found that the transverse shear modulus is in the order of 1/10 the longitudinal modulus. Accordingly, the above studies (taken together) suggest that the transverse instantaneous shear moduli of human skeletal muscles are in the order of 500 Pa to 2 KPa. No in vivo stress relaxation tests of skeletal muscles under transverse loading are available from humans, but stress relaxation in transversally loaded living tibialis anterior of rats showed that long-term relaxation forces are in the order of 0.5 to 0.6 the instantaneous force [46], and this was confirmed in stress relaxation tests obtained in the present study. Because shear moduli are linearly proportional to the relaxation force [Eq. (1)], it can be deduced that long-term transverse shear moduli of human skeletal muscles should be in the order of 250 Pa to 1200 Pa, in excellent agreement with G_∞ values reported herein for transversally loaded uninjured rat muscle tissue (range: 345 Pa to 730 Pa, Fig. 5). We therefore conclude that G_∞ values obtained from living rat gracilis muscles are suitable for representing human skeletal muscles in the present FE simulations.

Limitations of the present study lie with the assumption that tissues are homogenous and isotropic. This assumption was taken both during calculation of G_∞ from Eq. (1), and during computational modeling of the buttocks with the FE method. Indentation is an important biomechanical method because unlike standard uniaxial tension/compression mechanical testing it allows to determine properties of intact organs, which makes it applicable for use in vivo. While appreciating the experimental constraints of this in vivo method which cannot completely isolate the mechanical behavior of the tested muscle from those of adjacent, connected organs (e.g., viscoelastic responses of underlying tissues, or some motion at the joints of the animal's limb during indentation), our G_∞ measurements were repeatable and agreed very well with the literature, as described above. Thus, the simplification of muscle tissue as being homogenous and isotropic in Eq. (1) and utilization of the indentation method allowed to monitor muscle stiffening in vivo in our animal models. In the computational simulations, the assumption of homogeneity and isotropy of tissues was taken in lack of more detailed experimental data appropriate for the modeling; however, this compromise released considerable computational efforts for obtaining realistic, 3D stress analysis of the buttocks anatomy over time. Overall, the advantages of the coupled animal-computational modeling system outweigh the theoretical limitations.

The coupled animal-computer modeling system suggests that even 15 min of motionless sitting can cause some local damage to muscle tissue [continuous exposure to compressive stresses of 35 KPa–70 KPa as in Fig. 7 for 15 min was shown to induce cell death in rat gracilis as in Fig. 6(*b*)]. However, the 15 min time frame is less than that required to trigger the positive feedback mechanism of exacerbation in muscle regions subjected to moderate stresses [because the 35 KPa rat group did not show muscle stiffening after 15 min, Fig. 5(*a*)]. Immobilization for 30 min or over is expected to trigger the positive feedback mechanism across wide regions of muscle tissue (Fig. 8). Accordingly, the identification of the stiffening-stress-cell-death injury spiral developing during the initial 30 min of motionless sitting calls for reevaluation of the 1 h repositioning cycle recommended by the U.S. Department of Health [31]. The authors of this paper believe that shortening the cycle for patient repositioning is a key for minimizing PS in SCI, however, it seems impractical to manually reposition an immobilized, wheelchair-bounded patient in cycles on the order of several minutes. Automatic cushioning systems for wheelchairs (e.g., pressurized-air or fluid derived), however, can be programmed to produce these postural changes. Ultimately, individual SCI patients can be protected from PS by solving a patient-specific FE model of the buttocks subjected to (measured) buttocks-surface contact pressures. Comparison of the distributions of deep muscle tissue stresses and deformations (as function of posture) over time with muscle tissue injury thresholds from animal models will allow to identify the muscle regions susceptible to PS before actual injury occurs, and feed that information on real time to an automatic cushioning system for relieving deep muscle tissue stresses at the vulnerable sites.

Acknowledgments

The authors are thankful to the staff of the Injury Biomechanics Laboratory at the Department of Bioengineering of the University of Pennsylvania, PA: John Noon for designing and building the indentor; Brittany Coats for her technical assistance in preparing the indentation apparatus for the present study; Dr. Michele Hawk and Jill Ralston for their help in handling of animals prior to the indentation studies. We also appreciate the help of Dr. M. Scheinowitz, Dr. D. Castel, and S. Barzelai from the Neufeld Cardiac Research Institute of Sheba Medical Center, Israel in the handling of animals and conducting the dissections for the histology studies. Dr. S. Engelberg from the Laboratory for Vascular Biology, Sheba Medical Center is thanked for conducting and interpreting the histological analyses. Funding was provided by the Dan David Foundation (A.G.) and by the Internal Research Fund of Tel Aviv University (A.G.).

References

[1] Husain T., 1953, "An Experimental Study of Some Pressure Effects on Tissues, With Reference to the Bedsore Problem," J. Pathol. Bacteriol. **66**, pp. 347–358.
[2] Daniel, R. K., Priest, D. L., and Wheatley, D. C., 1981, "Etiologic Factors in Pressure Sores: An Experimental Model," Arch. Phys. Med. Rehabil. **62**, pp. 492–498.
[3] Knight, L. S., Taylor, P. R., Polliac, A. A., and Bader L. D., 2001, "Establishing Predictive Indicators for the Status of Loaded Soft Tissues," J. Appl. Physiol. **90**, pp. 2231–2237.
[4] Bouten, C. V., Breuls, R. G., Peeters, E. A., Oomens, C. W., and Baaijens, F. P., 2003, "In Vitro Models to Study Compressive Strain-Induced Muscle Cell Damage," Biorheology **40**, pp. 383–388.
[5] Allman, R. M., Goode, P. S., Patrick, M. M., Burst, N., and Bartolucci, A. A., 1995, "Pressure Ulcer Risk Factors Among Hospitalized Patients With Activity Limitation," JAMA, J. Am. Med. Assoc. **273**, pp. 865–870.
[6] National Spinal Cord Injury Statistical Center, 1997, "Annual Report for the Model Spinal Cord Injury Care Systems," University of Alabama, Birmingham, AL.
[7] Byrne D. W., and Salzberg C. A., 1996, "Major Risk Factors for Pressure Ulcers in the Spinal Cord Disabled: A Literature Review," Spinal Cord **34**, pp. 255–263.
[8] Tsokos, M., Heinemann, A., and Puschel, K., 2000, "Pressure Sores: Epidemiology, Medico-Legal Implications and Forensic Argumentation Concerning Causality," Int. J. Legal Med. **113**, pp. 283–287.
[9] Margolis, D. J., Knauss, J., Bilker, W., and Baumgarten, M., 2003, "Medical Conditions as Risk Factors for Pressure Ulcers in an Outpatient Setting," Age Ageing **32**, pp. 259–264.
[10] Bouten, C. V., Oomens, C. W., Baaijens, F. P., and Bader, D. L., 2003, "The Etiology of Pressure Ulcers: Skin Deep or Muscle Bound?," Arch. Phys. Med. Rehabil. **84**, pp. 616–619.
[11] Bliss, M. R., 1993, "Aetiology of Pressure Sores," Rev. Clin. Gerontol. 3, pp. 379–397.
[12] Smith, P. W., Black, J. M., and Black, S. B., 1999, "Infected Pressure Ulcers in the Long-Term-Care Facility," Infect. Control Hosp. Epidemiol. **20**, pp. 358–361.
[13] Smith, J. W., 1954, "Elastic Properties of the Anterior Cruciate Ligament of the Rabbit," J. Anat. **88**, pp. 369–380.
[14] Fitzgerald, E. R., and Freeland, A. E., 1970, "Viscoelastic Response of Intervertebral Discs at Audio Frequencies," Med. Biol. Eng. **9**, pp. 459–478.
[15] Rang, E. M., Lippert, S. A., and Grimm, M. J., 2001, "The Degradation of Material Properties of Brain Tissue as a Function of Time Postmortem," *Proceedings of the Summer ASME Bioengineering Conference*, Snowbird, Utah, June 27–July 1, University of Toledo, OH, pp. 887–888.
[16] Hayes, W. C., and Bodine, A. J., 1978, "Flow-Independent Viscoelastic Properties of Articular Cartilage Matrix," J. Biomech. **11**, pp. 407–419.
[17] Goll, D. E., Taylor, R. G., Christiansen, J. A., and Thompson, V. F., 1992, "Role of Proetinases and Protein Turnover in Muscle Growth and Meat Quality," *Procecdings 44th Annual Recip. Meat Conference*, National Livestock and Meat Board, Chicago, IL, American Meat Science Association (AMSA), Savoy, IL, pp. 25–36.
[18] Mayer, R. G., and Bigelow, G. S., 1990, *Embalming: History, Theory, and Practice*, Appleton and Lange, East Norwalk, CT.
[19] Linder-Ganz, E., and Gefen, A., 2004, "Mechanical Compression-Induced Pressure Sores in Rat Hind-Limb: Muscle Stiffness, Histology and Computational Models," J. Appl. Physiol. **96**, pp. 2034–2049.
[20] Kovanen, V, Suominen, H, and Heikkinen, E., 1984, "Mechanical Properties of Fast and Slow Skeletal Muscle With Special Reference to Collagen and Endurance Training," J. Biomech. **17**, pp. 725–735.
[21] Vankan, W. J., Huyghe, J. M., van Donkelaar, C. C., Drost, M. R., Janssen, J. D., and Huson, A., 1998, "Mechanical Blood-Tissue Interaction in Contracting Muscles: A Model Study," J. Biomech. **31**, pp. 401–409.
[22] Lai-Fook, S. J., Wilson, T. A., Hyatt, R. E., and Rodarte, J. R., 1976, "Elastic Constants of Inflated Lobes of Dog Lungs," J. Appl. Physiol. **40**, pp. 508–513.
[23] Vannah, W. M, and Childress, D. S., 1996, "Indentor Tests and Finite Element Modeling of Bulk Muscular Tissue In Vivo," J. Rehabil. Res. Dev. **33**, pp. 239–252.
[24] Gefen, A., Megido-Ravid, M., Azariah, M., Itzchak, Y., and Arcan, M., 2001, "Integration of Plantar Soft Tissue Stiffness Measurements in Routine MRI of the Diabetic Foot," Clin. Biomech. (Los Angel. Calif.) **16**, pp. 921–925.
[25] Gefen, A., Gefen, N., Zhu, Q., Raghupathi, R., and Margulies, S. S., 2003, "Age-Dependent Changes in Material Properties of the Brain and Braincase of the Rat," J. Neurotrauma **20**, pp. 1163–1177.
[26] Gefen, A., and Margulies, S. S., 2004, "Are In Vivo and In Situ Brain Tissues Mechanically Similar?," J. Biomech. **37**, pp. 1339–1352.
[27] Lee, E. H., and Radok, J. R. M., 1960, "The Contact Problem for Viscoelastic Bodies," ASME J. Appl. Mech. **27**, pp. 438–444.
[28] Zheng, Y., Mak, A. F., and Lue, B., 1999, "Objective Assessment of Limb Tissue Elasticity: Development of a Manual Indentation Procedure," J. Rehabil. Res. Dev. **36**, pp. 71–85.
[29] Newson T. P., and Rolfe, P., 1982, "Skin Surface PO2 and Blood Flow Measurements Over the Ischial Tuberosity," Arch. Phys. Med. Rehabil. **63**, pp. 553–556.
[30] Patterson, R. P., and Fisher, S. V., 1980, "Pressure and Temperature Patterns Under the Ischial Tuberosities," Bull. Prosthet. Res. **10-34**, pp. 5–11.
[31] Agency for Health Care Policy and Research (AHCPR, 1994, "Treatment of Pressure Ulcers" in *Clinical Practice Guideline No. 15*, U.S. Department of Health and Human Services, Publication No. 95-0652, Washington, DC.
[32] Kosiak, M., 1961, "Etiology of Decubitus Ulcers," Arch. Phys. Med. Rehabil. **42**, pp. 19–29.
[33] Salcido, R., Fisher, S. B., Donofrio, J. C., Bieschke, M., Knapp, C., Liang, R., LeGrand, E. K., and Carney, J. M., 1995, "An Animal Model and Computer-Controlled Surface Pressure Delivery System for the Production of Pressure Ulcers," J. Rehabil. Res. Dev. **32**, pp. 149–161.
[34] Peirce, S. M., Skalak, T. C., and Rodeheaver, G. T., 2000, "Ischemia-Reperfusion Injury in Chronic Pressure Ulcer Formation: A Skin Model in the Rat," Wound Repair Regen **8**, pp. 68–76.
[35] Bosboom, E. M., Bouten, C. V., Oomens, C. W., van Straaten, H. W., Baaijens, F. P., and Kuipers, H., 2001, "Quantification and Localisation of Damage in Rat Muscles After Controlled Loading; A New Approach to Study the Aetiology of Pressure Sores," Med. Eng. Phys. **23**, pp. 195–200.
[36] Drerup B., Kraneburg, S., Koller, A., 2001, "Visualisation of Pressure Dose: Synopsis of Peak Pressure, Mean Pressure, Loading Time and Pressure Time-Integral," Clin. Biomech. (Los Angel. Calif.) **16**, pp. 833–834.
[37] Carew, E. O., Barber, J. E., and Vesely, I., 2000, "Role of Preconditioning and Recovery Time in Repeated Testing of Aortic Valve Tissues: Validation Through Quasilinear Viscoelastic Theory," Ann. Biomed. Eng. **28**, pp. 1093–1100.
[38] Zhang, M., and Mak, A. F., 1999, "In Vivo Friction Properties of Human Skin," Prosthet. Orthot Int. **23**, pp. 135–141.
[39] Tschoegl, N. W., 1989, *The Phenomenological Theory of Linear Viscoelastic Behavior: An Introduction*, Springer, New York.
[40] Hamhaber, U., Grieshaber, F. A., Nagel, J. H., and Klose, U., 2003, "Comparison of Quantitative Shear Wave MR-Elastography With Mechanical Compression Tests," Magn. Reson. Med. **49**, pp. 71–77.
[41] Fridén J, and Lieber R. L., 2003, "Spastic Muscle Cells Are Shorter and Stiffer Than Normal Cells," Muscle Nerve **27**, pp. 157–164.
[42] Basford, J. R., Jenkyn, T. R., An, K. N., Ehman, R. L., Heers, G., and Kaufman K. R., 2002, "Evaluation of Healthy and Diseased Muscle With Magnetic Resonance Elastography," Arch. Phys. Med. Rehabil. **83**, pp. 1530–1536.
[43] Uffmann, K., Maderwald, S., Ajaj, W., Galban, C. G., Mateiescu, S., Quick, H.

H., and Ladd, M. E., 2004, "In Vivo Elasticity Measurements of Extremity Skeletal Muscle With MR Elastography," NMR Biomed. **17**, pp. 181–190.
[44] Dresner, M. A., Rose, G. H., Rossman, P. J., Muthupillai, R., Manduca, A., and Ehman, R. L., 2001, "Magnetic Resonance Elastography of Skeletal Muscle," J. Magn. Reson Imaging **13**, pp. 269–276.
[45] Gennisson, J.-L., Catheline, S., Chaffaï, S., and Fink, M., 2003, "Transient Elastography in Anisotropic Medium: Application to the Measurement of Slow and Fast Shear Wave Speeds in Muscles," J. Acoust. Soc. Am. **114**, pp. 536–541.
[46] Bosboom, E. M, Hesselink, M. K, Oomens, C. W., Bouten, C. V., Drost, M. R., Baaijens, F. P., 2001, "Passive Transverse Mechanical Properties of Skeletal Muscle Under In Vivo Compression," J. Biomech. **34**, pp. 1365–1368.